Silvio Francisco Brunatto
brunatto@ufpr.br
Departamento de Engenharia Mecânica
Universidade Federal do Paraná (UFPR)
81531-990 Curitiba, PR, Brazil

Plasma Assisted Parts' Manufacturing: Sintering and Surface Texturing – Part I – Influence of Sintering Time and Temperature

The acquirements and potentiality universe of cleaning, heating and/or sputtering effects caused by plasma species bombardment phenomenon on the surface characteristics and finishing of manufactured parts treated in DC abnormal glow discharge opens a new research and development field, called here of Plasma Assisted Parts' Manufacturing (PAP'M). The adequate control of the sputtering mechanism allows the production of different kinds of surface. Therefore, the design of rough or smooth surface, presenting a modified distribution of surface porosity and texturing could be idealized, in accordance with the desired surface characteristics, as the parts are simultaneously sintered and treated. The first part (out of two) of this work performed in hollow cathode discharge (HCD) presents the results of the surface morphology's changes in the pressed iron samples and in the internal surfaces of the external cathodes as a function of the sintering time and temperature. Potential applications include small diameters' cylindrical parts and components like axles, pins, pivots, and tubes and pipes presenting small internal diameters. Sputtering effects were quantified by means of mass loss and Ra and Rz roughness measurements and qualified by means of SEM. The overall work comprises the study of different parameters, including sintering time and temperature (Part I), and inter-cathode distance and pressure (Part II). Results indicate the sputtering mechanism in HCD sintering and surface texturing treatments could be adequately controlled as a function of the plasma parameters, comprising an important contribution to the development of green technologies for surface texturing, surface engineering, and part's manufacturing.

***Keywords**: Plasma Assisted Parts' Manufacturing (PAP'M), Hollow Cathode Discharge (HCD), plasma sintering, surface texturing, sputtering, sintering time, sintering temperature*

Introduction

The use of DC plasma in the metallic materials processing has increased steadily in recent years. The possibility of altering the material surface's characteristics by exposing it to the plasma species has led to the development of new techniques and applications (nitriding, sputtering, deposition, sintering…), which have demanded special attention of researchers in the metallurgical-mechanical field (Brunatto et al., 2008).

In the sintering of metallic components using an abnormal glow discharge containing hydrogen and argon, the pressed sample to be sintered is placed inside the cathode, and sufficiently high temperatures can be reached to sinter metals by bombarding the cathode with plasma (ion and neutral) species (Muzart et al., 1997).

Hollow cathode discharge (HCD) in abnormal regime is a variant of the abnormal glow discharge technique, whose cathode geometry produces a discharge of higher ionization rate (v. Engel, 1994). As a result of an intense cathode bombardment by ions and fast neutrals, an increased heating efficiency is obtained in the same proportion as compared to the linear discharge. This kind of discharge occurs in cathodes presenting cavities or hollows (see Fig. 1), when the discharge fills the cavity under given conditions governed by the "a x p" product (a: inter-cathode distance; and p: gas pressure). In practice, considering the possible geometries and arrangements, the hollow cathode effect occurs for "a x p" products ranging from 0.375 to 3.75 cm Torr (Koch et al., 1991).

The hollow cathode effect also causes an increase of the current density at low pressures (normally between 1 and 9 Torr, in accordance with Brunatto et al. (2008), in response to an exponential multiplication of electrons produced by ionization in cathode sheaths (Kolobov and Tsendin, 1995). This effect is accomplished by increasing both the secondary electron emission rate and through the sputtering mechanism (Benda et al., 1997; Koch et al., 1991). Considering practice aspects and technological interests, besides the high heating efficiency, an intense sputtering mechanism can be expected using HCD. In addition, sputtering on cathodes' surface could be related to two different effects: a) the amount of metallic atoms sputtered, backscattered or diffused into the glow and deposited on the surfaces (in accordance with Brunatto and Muzart, 2007); and b) the modification of the surfaces' morphology.

The above-mentioned aspects indicate the metallic parts processed by means of DC abnormal glow discharge present characteristics that are directly related to the cleaning, heating and/or sputtering effects caused by plasma species (ions and neutrals) bombardment phenomenon. The acquirements and potentiality universe of these effects on the manufactured parts' surface characteristics are far-away from being finished. So, a new research and development field could be evidenced, which is called here of Plasma Assisted Parts' Manufacturing (PAP'M). In such case, considering the classical steps that involve the manufacture of a mechanical component (design, structural calculus, material selection and specification, production, and quality control), according to our understanding, the manufacturing planning must necessarily consider the effects caused by the plasma species bombardment on the parts surface. One of them is specially considered in this work, i.e. the sputtering effect. The adequate control of the sputtering mechanism can allow the obtainment of different kinds of surface. So, the design of rough or smooth surface, presenting a modified distribution of surface porosity could be idealized in accordance with the desired surface characteristics.

In this study performed in hollow cathode discharge (HCD), the first results of the surface morphology's changes in the pressed

Paper accepted December, 2009. Technical Editor: Anselmo Eduardo Diniz

cylindrical iron samples and in the internal surfaces of external cathodes are presented as a function of the sintering time and temperature. Two aspects were emphasized: a) the superficial pores' morphology modification in pressed samples processed by HCD, which could be explored as a new way to perform sintering and surface texturing treatments in small diameters cylindrical parts like axles, pins, and pivots (the study of the chemical composition modification of the iron sample's surface is not considered here, since it is presented in previous work, Brunatto et al., 2005); and b) in the internal surface of the external cathode, which acts as a pipe (see Fig. 1), the mechanism of the metallic atoms deposition, altering its start chemical composition and the surface morphology via HCD, which could be explored as a new way to perform deposition and surface texturing treatments in pipes presenting small internal diameters. Sputtering effects are quantified by means of mass loss measurements and qualified by means of SEM. Measurements of roughness are presented too. The overall work comprises the study of different parameters, including the influence of sintering time and temperature (Part I), and inter-cathode distance and pressure (Part II), indicating the sputtering mechanism could be adequately controlled to attend the premise and comprising an important contribution to the development of green technologies for surface texturing, surface engineering, and consequently for part manufacturing.

Nomenclature

Ar = *argon*
DC = *Direct Current*
HCD = *Hollow Cathode Discharge*
H_2 = *hydrogen*
PAP'M = *Plasma Assisted Parts' Manufacturing*
SEM = *Scanning Electron Microscopy*
ton = *switched-on pulse time*
a = *inter-cathode distance*
p = *gas pressure*
Ra = *roughness Ra*
Rz = *roughness Rz*

Experimental Procedure

Figure 1 consists of an "in situ" view of the plant in use showing the hollow cathode discharge and both the cathodes. Detailed representation of the experimental apparatus is available in the earlier reports (Brunatto and Muzart, 2007).

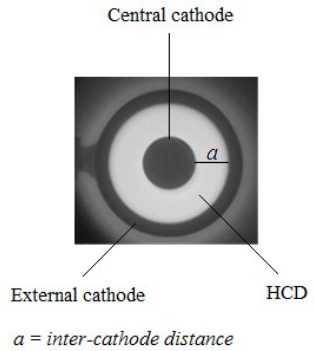

Figure 1. An "in situ" view of the plant in use showing the hollow cathode discharge and both the cathodes.

The discharge chamber consisted of a 350 mm diameter, 380 mm high stainless steel cylinder attached to steel plates and sealed with o-rings at both ends. The system was evacuated to a residual pressure of 1.33 Pa using a two stage mechanical pump. The gas mixture of Ar and H_2 was adjusted by two mass flow controllers of 8.33 x 10^{-6} and 3.33 x 10^{-6} m^3s^{-1} operating at full scale, for Ar and H_2 gas, respectively. The pressure in the vacuum chamber was adjusted with a manual valve and measured with a capacitance manometer of 1.33 x 10^3 Pa (10 Torr) in full-scale operation.

A sample of 9.5 mm diameter and 10 mm height was placed on an AISI 1008 carbon steel support (12 mm height) that served as the central cathode. A cylindrical low carbon steel part (3.5 mm height) was placed at the top of the sample in order to generate a homogeneous annular discharge. The external cathode was machined from an AISI 310 stainless steel tube (atomic % composition: 25.0% Cr, 16.0% Ni, 1.5% Mn, 1.5% Si, 0.03% C and the balance, Fe) of internal diameter of 21.2 mm, 2 mm wall thickness and 25.4 mm height. The internal surfaces of the external cathodes were handy finished by polishing using 1200 grade sand-paper in high rotation machine.

Both cathodes were negatively biased at the same voltage, using a square form pulsed power supply. The voltage was set to 565 V. To ensure a stable discharge, an electrical resistance was connected in series between the power supply and the discharge chamber. The power transferred to the plasma was adjusted by varying the time that the pulse was switched on (ton). The pulse period used was 200 μs. For the sintering time study the temperature of the sample was selected in 1423 K (1150 °C) by adjusting the on/off time of the pulsed voltage. The ton values applied to the cathodes decreased slightly from 44 and 39 μs for sintering times ranging from 30 to 240 min, in accordance with Brunatto et al. (2005). For the sintering temperature study the ton values applied to the cathodes were 35, 41 and 50 μs (these values correspond to the average of the last 20 min at the sintering stage), and the central cathode current and the total current (central cathode plus external cathode current) were 131, 160 and 193 mA, and 390, 458 and 544 mA, in order to obtain sintering temperatures of 1323, 1423 and 1523 K (1050, 1150 and 1250 °C), respectively. The temperature was measured by means of a chromel–alumel (type K of 1.5 mm diameter) thermocouple inserted to a depth of 8 mm into the sample holder.

Samples of unalloyed iron were produced using Ancorsteel 1000C iron powder (99.75 wt% pure). A double action press with moving die body was used to press the samples, which had a green density of 7.0 ± 0.1 gcm^{-3}. The mass of the pressed samples was typically around 5.0 g. The mass loss of the samples was measured with a 0.1 mg precision balance.

Sintering was performed at 1423 K (1150 °C) for times of 30, 60, 120, and 240 min, at pressure of 400 Pa (3 Torr), inter-cathode distance of 5.8 mm, with a gas flow of 5 x 10^{-6} m^3s^{-1} (in accordance with Brunatto and Muzart, 2007), and a gas mixture composed of 80% Ar and 20% H_2. The same was applied to the sintering at 1323, 1423 and 1523 K (1050, 1150 and 1250 °C) for time of 60 min. The sintering procedure was divided into three steps:

a) The samples were cleaned under a discharge at 723 K (450 °C) for 30 min, using 133 Pa (1 Torr) pressure and the resistance adjusted to 100 Ω;

b) They were heated at a heating rate of 0.42 Ks^{-1} (0.42 $°Cs^{-1}$) and sintered at 1423 K (1150 °C), using 400 Pa (3 Torr) pressure and resistance adjusted to 50 Ω;

c) The samples were cooled under a gas mixture flow.

Characterization was carried out on the sample's cylindrical surface and on the internal cylindrical surface of the external cathode, which are the surfaces exposed to the exponential glow discharge. The surface morphology of the samples was characterized by means of scanning electron microscopy, using a Philips XL-30 microscope. The chemical composition of the surfaces was obtained by means of energy dispersive x-ray

microprobe analysis. Sputtering effects were quantified by means of mass loss and roughness determination. Measurements of roughness were conducted in accordance with ISO 4287 (1997) for Ra and Rz determination, using Mahr (Concept) equipment, filter Gauss, and 400 µm measurement length and 80 µm wave length (five divisions) for the sintered samples, and 4 mm measurement length and 0.80 mm wave length (five divisions) for the internal surfaces of the external cathode. Mathematically, Ra is the arithmetic average value of the profile departure from the mean line within a sampling length and is given by the sum of the absolute values of all the areas above and below the mean line divided by the sampling length, and Rz is the maximum height of profile (peak to valley) within a sampling length, and is usually analyzed as an average of the 5 values comprising the highest value for peak to valley distance taken in each division in the sampling length.

Results and Discussion

Aspects Related to the Sintering Time

a) In the Cylindrical Surface of the Iron Samples

Surface finish aspects of the iron samples sintered in HCD are shown in Fig. 2. To emphasize the effects of the ion bombardment on the surface characteristics of the samples, a same place was characterized by SEM before (in the pressed or green state – Fig. 2: a1, b1, c1, and d1) and after plasma exposition (in the sintered state – Fig. 2: a2, b2, c2, and d2), for 30, 60, 120 and 240 min sintering times, respectively. Two different aspects can be observed: a) the surface finishing modification; and b) the superficial pores' morphology modification. The first aspect is related to the confrontation of the results shown in the Fig. 2 (a2, b2, c2, d2), which indicates a strong modification of the surface finishing as a function of the sintering time. The changes in the surface finishing can be explained by the intense sputtering mechanism caused by ion bombardment phenomenon on the surfaces exposed to the plasma in the HCD, resulting in the sputtering of iron atoms from the sample surface.

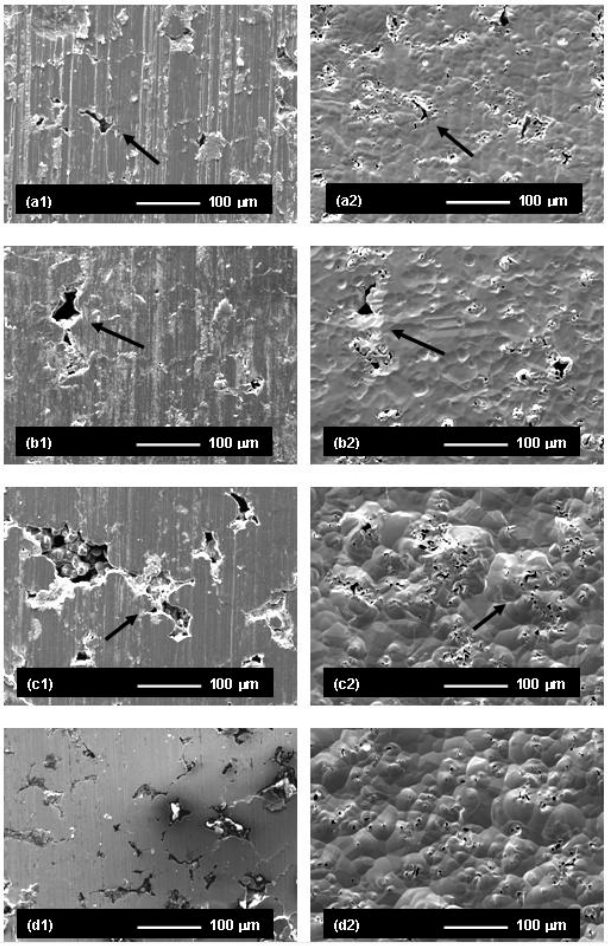

Figure 2. Surface finishing aspects of the iron samples: a1, b1, c1, and d1) in the pressed state; and a2, b2, c2, and d2) after plasma exposition, for 30, 60, 120 and 240 min sintering times, respectively.

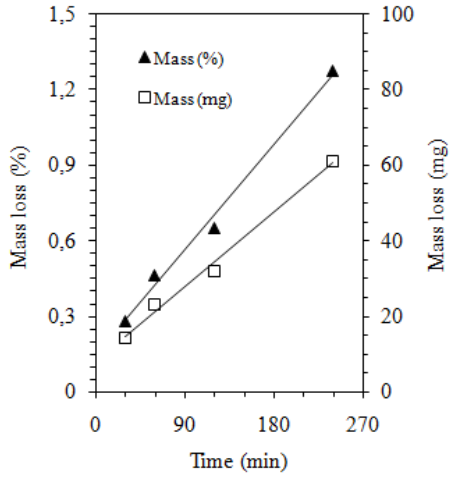

Figure 3. Mass loss measurements of the iron samples processed for different sintering times.

Figure 3 shows the mass loss measurements of the samples, taken to evaluate the sputtering effect on the central cathode according to the sintering time. The mass losses ranged from 0.28% to 1.26% (14 - 63 mg), confirming the intense sputtering that occurred in the central cathode. It is to be noted that the use of higher sintering times cause the enhancement of the surface changes in relation to the start surface condition (see Fig 2: a1 x a2, b1 x b2, c1 x c2, d1 x d2). The data shown in Fig. 3, comprising the mass loss (y) given in % unit, were mathematically treated to evaluate the mass loss for different sintering times (x) given in min unit. The equation of the fitted curve was:

$$y = 0.004x + 0.145 \qquad (R^2 = 0.992) \qquad (1)$$

Figure 4 shows the Ra and Rz roughness measurements of the samples, taken to evaluate the surface changes as a consequence of the sputtering effects on the central cathode according to the sintering time. The Ra and Rz ranged from 0.37 to 0.77 µm and from 1.81 to 3.18 µm, respectively, for sintering times ranging from 30 to 240 min, confirming the enhancement of the surface modification and the results previously obtained by SEM (Fig 2: a2, b2, c2, d2).

The second aspect is related to the confrontation of the results shown in Fig. 2 (a1 x a2, b1 x b2, c1 x c2, d1 x d2). It is important to note that the sputtering effect tends to promote significant changes on the superficial pores' morphology, considering the start pores present in the pressed samples' cylindrical surfaces. Note that slight changes in the surface finishing and in the open pore's

apparent volume can be observed for the 30 min sintering time processed sample (Fig. 2: a1 x a2). Otherwise, the higher the sintering time, the higher was the change on the superficial pores' morphology. The results shown in Fig. 2 (b1 x b2, c1 x c2, d1 x d2) clearly indicate the open pores tend to became closed as a consequence of the intense material transport mechanism verified for the metallic atoms, by interactions in the plasma-surface system. So, a tendency of surface modification in the pore size distribution could be expected increasing the sintering time, which would lead to a fine and disperse distribution of small open pores, in accordance with the results shown in Fig.2 (d1 x d2) and considering the parameters studied. The results presented here indicate the hollow cathode discharge could be applied to develop a new green technology for surface texturing, becoming a new technique to improve surface properties such as roughness and morphology. These properties are important parameters for many applications directly related to the coatings adhesion, tribological performance, and others, in accordance with Gupta et al. (2007), Basnyat et al. (2008), and Krupka et al. (2008).

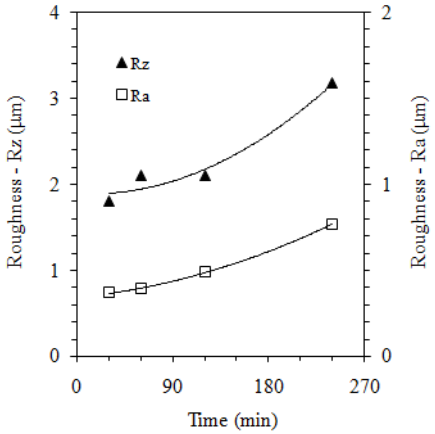

Figure 4. Ra and Rz roughness measurements of the iron samples processed for different sintering times.

b) In the Internal Surface of the External Cathodes

Surface finish aspects of the internal surface of the external cathodes processed in HCD are shown in Fig. 5. To emphasize the effects of the sputtering on the characteristics of the internal surface as a function of the processing time, results are compared with the start surface condition (Fig. 5e), which was obtained by polishing. The results indicate that the surface morphology is strongly modified. For short sintering times (30 and 60 min, Fig. 5a and 5b, respectively) two different textured surfaces can be observed. Both the surfaces are characterized by the presence of round micrometer particles, which are probably formed from the deposition of metallic atoms clusters plus ions formed at plasma phase and subsequent coagulation or sintering on the surface. This assumption is based in the results of Romanowsky and Wronikowsky (1992), which observed the obtainment of a deposit layer with a typical morphology of powder particles in a study comprising the application of the reactive pulsed plasma technique.

According to the chemical analysis of the internal surface of the external cathodes (Table 1), the increase in the Fe contents and consequent decrease in the amount of Cr, Ni, Si and Mn indicates that the Fe atoms sputtered from the pressed iron samples (see results discussed in Fig. 2) diffuse into the plasma and condense on the internal surface of the external cathode. The higher the sintering time, the higher is the amount of iron atoms altering the chemical composition of the surrounding surface.

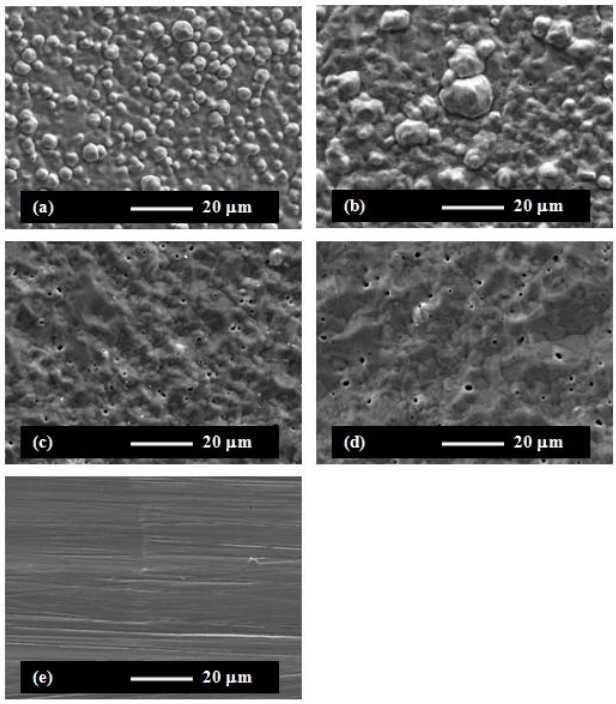

Figure 5. Surface finish aspects of the internal surface of the external cathodes processed in HCD for sintering times of: a) 30 min; b) 60 min; c) 120 min; d) 240 min; and e) in the as non-processed condition.

The round particles shape verified in Fig. 5(a, b) is probably due to the high processing temperature. As known, the atomic diffusion in solid state increases with temperature, and a decreasing in the surface free-energy can be expected for the round shape, since the spherical shape has a minimum area/volume ratio. Although the external cathode temperature was not monitored, the heat irradiated from the central cathode (at 1150 °C) and the heat produced by ion bombardment effect indicate the temperature of the internal surface of the external cathode is very close for that verified to the central cathode. A study by Timanyuk and Tkachenko (1989) supports this affirmation. Their findings revealed that the dark space in the central cathode of an annular discharge is thinner than that observed on the internal surface of the external cathode. Therefore, fewer collisions between ions and neutral species tend to occur in the central cathode sheath, resulting in higher kinetic energy of the incident ions, higher heating effect and, hence, higher sputtering yield of the sample surface. Moreover, another result to be explained is the difference of the particles' size and distribution verified for both the surfaces.

Figure 5(a) shows a texture comprising fine and homogeneous particles dispersion. The increase of the sintering time resulted in particle growth and in a non-homogeneous dispersion (Fig. 5b), which could be associated to the particles coalescence phenomenon, as a consequence of an intense surface diffusion activated by ion bombardment effect. Finally, it is important to note the presence of argon in the composition of the processed surfaces even for short sintering times (Table 1). The presence of argon retained on the metallic surface would confirm the above mentioned assumption, which is a strong indicative that ions participate in the formation of the condensed particles. Otherwise, for long sintering times (120 and 240 min, Figs. 5c and 5d, respectively) new changes in the surface morphology can be observed. The round particle texture observed for short sintering times disappears.

Table 1. Average concentrations and standard deviation of Cr, Ni, Si, Fe and Ar measured on the internal surface of the external cathodes processed with different sintering times (Manganese was not met).

Sintering time (min)	Chromium (at.%)	Nickel (at.%)	Silicon (at.%)	Iron (at.%)	Argon (at.%)
as non-processed	25.8 + 0.5	16.0 + 0.4	1.5 + 0.1	55.2 + 0.5	0
30	17.7 + 1.2	9.0 + 0.7	0.8 + 0.1	71.6 + 1.0	0.9 + 0.1
60	14.8 + 1.4	7.3 + 0.6	0.7 + 0.1	74.9 + 1.1	1.3 + 0.1
120	14.5 + 1.5	5.7 + 0.7	0.6 + 0.1	77.2 + 1.2	2.0 + 0.1
240	12.6 + 1.1	3.8 + 0.4	0.4 + 0.1	81.1 + 0.8	2.1 + 0.2

Figure 6 shows the Ra and Rz roughness measurements of the internal surfaces as a function of the sintering time, taken to evaluate the surface changes as a consequence of the sputtering effects on the external cathodes. The Ra and Rz ranged from 0.43 to 0.84 μm and from 4.51 to 7.36 μm, respectively. For short sintering times (30 and 60 min, Figs. 5a and 5b) the Ra and Rz values are quite similar, ranging between 0.60 ± 0.02 μm and 4.99 ± 0.03 μm, respectively. The slight decrease of the Ra and Rz values for 0.43 and 4.51 μm, respectively, verified for surfaces processed with 120 min times (see Fig. 6), indicates the round-particle atoms tend to dissolve into surface.

Another event that occurs simultaneously is the re-sputtering of the particle atoms, since both the surfaces in the annular discharge are submitted to the ion bombardment effect. In accordance with the results verified for 30, 60 and 120 min sintering time presented in Fig. 5(a, b, c) and in Fig. 6, it is possible to assume the surface texturing process considering the particle deposition is completed for 120 min sintering time. The increase of the sintering time to 240 min leads to increase substantially the Ra and Rz values of the surface, for 0.84 and 7.36 μm respectively, as a consequence of the ion bombardment effect (see Fig. 5d).

Finally, for long sintering times (Fig. 5c, d), another characteristic tends to present at surface, since nanometric and micrometric porosity appears. This fact is probably related to the presence of argon atoms from the gaseous mixture dissolved into surface. In addition, the intense ion bombardment effect would tend to increase the point crystalline defects and an increment in the vacancy density could be expected. The argon atom-vacancy pair diffusion could result in the coalescence of them at surface, leading to the formation of new and small porous. This event would allow describing a new kind of surface texturing, which could be useful to store liquid lubricants and present beneficial effects of surface texturing, like that verified on mixed lubricated contacts, in accordance with Krupka et al. (2008) study.

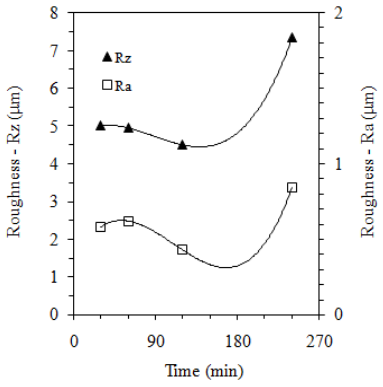

Figure 6. Ra and Rz roughness measurements of the internal surfaces of the external cathodes processed for different sintering times.

Aspects Related to the Sintering Temperature

a) In the Cylindrical Surface of the Iron Samples

Surface finish aspects of the iron samples sintered in HCD are shown in Fig. 7. To emphasize the effects of the ion bombardment on the surface characteristics of the samples, a same place was characterized by SEM before (in the pressed or green state – Fig. 7: a1, b1, and c1) and after plasma exposition (in the sintered state – Fig 7: a2, b2, and c2), for 1323, 1423 and 1523 K (1050, 1150 and 1250 °C) sintering temperatures, respectively.

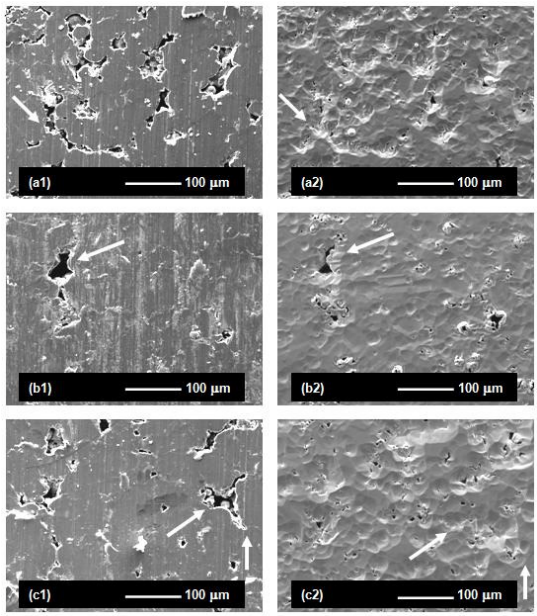

Figure 7. Surface finish aspects of the iron samples: a1, b1, and c1) in the pressed state; and a2, b2, and c2) after plasma exposition, for 1050, 1150, and 1250 °C, respectively.

Two different aspects can be observed: a) the surface finishing modification; and b) the superficial pore morphology modification. The first aspect is related to the confrontation of the results shown in Fig. 7 (a2, b2, c2), which indicate the modification of the surface finishing is dependent on the sintering temperature. The changes in the surface finishing can be explained by the intense sputtering mechanism caused by ion bombardment phenomena on the samples surface exposed to the plasma in the HCD, resulting in the sputtering of iron atoms from the sample surface. It is important to emphasize, despite the sintering time (60 min), the pressure (3 torr), the inter-cathode space (5.8 mm), the gas flow (5×10^{-6} m^3s^{-1}), and the discharge voltage (570 V) are the same. Higher sintering

temperatures were obtained increasing the ton values applied to the cathodes, in accordance with the data presented in the experimental procedure (35, 41 and 50 μs ton for sintering temperatures of 1323, 1423 and 1523 K, respectively). The higher the ton, the higher is the effective time the electrical discharge works, resulting in a longer ion bombardment effect applied to the exposed surfaces.

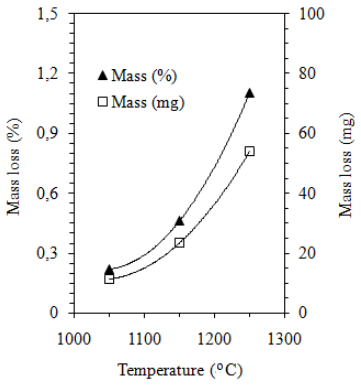

Figure 8. Mass loss measurements of the iron samples processed for different temperatures.

Figure 8 shows the mass loss measurements of the samples, taken to evaluate the sputtering effect on the central cathode according to the sintering temperature. The mass losses were 0.22, 0.46 and 1.10% (11, 23 and 54 mg) for 1050, 1150 and 1250 °C sintering temperatures, respectively. The data shown in Fig. 8 were mathematically treated to evaluate the mass loss (y) given in % unit for different sintering temperatures (x) given in °C unit. The equation of the fitted curve resulting in an exponential approach was:

$$y = 0.00005\, e^{0.008x} \qquad (R^2 = 0.997) \qquad (2)$$

This result differs from the previously observed in Eq. (1), which has considered the sintering time as a study parameter (x, in min). It is to be noted that the sputtering effects on the sample mass loss for 1050 °C and 60 min condition (presenting a mass loss of 0.22%) is similar for that obtained at 1150 °C and 30 min (with mass loss of 0.28%). Using Eq. (1), a mass loss of 0.22% could be obtained from a sintering time of 19 min (calculated value), at 1150 °C condition. In other words, for mass losses' similar results, an increment in 100 °C (from 1050 to 1150 °C) to the sintering temperature would lead to a decreasing on the order of 68% (from 60 to 19 min) in the sintering time. The same mathematical treatment was repeated for the 1250 °C and 60 min condition, which evidenced a mass loss of 1.10%. In such case, similar result was verified for the 1150 °C and 240 min sintering time condition (presenting a mass loss of 1.27%). Using Eq. (2), a mass loss of 1.27% could be obtained from a sintering temperature of 1268 °C (calculated value), at 60 min condition. In other words, for mass losses' similar results, an increment in 118 °C (from 1150 to 1268 °C) to the sintering temperature would lead to a decreasing of the order of 75% (from 240 to 60 min) in the sintering time.

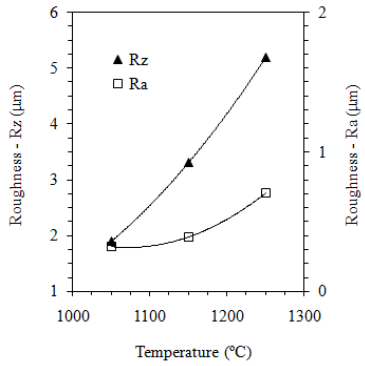

Figure 9. Ra and Rz roughness measurements of the iron samples processed for different temperatures.

In addition, the use of higher sintering temperatures causes the enhancement of the surface changes in relation to the start surface condition (see Fig 7: a1 x a2, b1 x b2, c1 x c2).

Figure 9 shows Ra and Rz roughness measurements of the samples, taken to evaluate the surface changes as a consequence of the sputtering effects on the central cathode, according to the sintering temperature. The Ra and Rz values were 0.32, 0.39 and 0.77 μm, and 1.9, 3.3 and 5.2 μm for sintering temperatures of 1050, 1150 and 1250 °C, respectively, confirming the enhancement of the surface modification and the results previously obtained by SEM (Fig 7: a2, b2, c2).

The second aspect is related to the confrontation of the results shown in Fig. 7 (a1 x a2, b1 x b2, c1 x c2). It is important to observe that the sputtering effect tends to promote changes on the superficial pores' morphology, considering the start pores present in the pressed samples' cylindrical surfaces.

Significant modifications in the surface finishing and in the open pores apparent volume can be observed for the 1050 °C sintering temperature processed sample (Fig. 7: a1 x a2). It should be noted that the alterations of the superficial pores morphology were congruent with the mass loss measurements, both being dependent on the sintering temperature. In addition, the open pores tend to became closed as a consequence of the intense material transport mechanism verified for the metallic atoms, by the interactions in plasma-surface system. So, a tendency of surface modification in the pore size distribution could be expected increasing the sintering temperature, which would lead to a fine and disperse distribution of small open pores, considering the parameters studied. Otherwise, in Fig.7 (b1 x b2) is evidenced the successes in closing open pores is strongly dependent on the start pore size besides the electrical discharge parameters. The results presented here indicate the hollow cathode discharge could be applied to develop a new green technology for surface texturing, becoming a new technique to improve surface properties such as roughness and morphology. These properties are important parameters for many applications directly related to the coatings adhesion, tribological performance, and others, in accordance with Gupta et al. (2007), Basnyat et al. (2008), and Krupka et al. (2008).

Table 2. Average concentrations and standard deviation of Cr, Ni, Si, Fe and Ar measured on the internal surface of the external cathodes processed with different sintering temperatures (Manganese was not met).

Sintering temperature (°C)	Chromium (at.%)	Nickel (at.%)	Silicon (at.%)	Iron (at.%)	Argon (at.%)
as non-processed	25.8 + 0.5	16.0 + 0.4	1.5 + 0.1	55.2 + 0.5	0
1050	16.1 + 1.0	8.6 + 1.1	0.8 + 0.1	74.1 + 1.0	0.4 + 0.1
1150	14.8 + 1.4	7.3 + 0.6	0.7 + 0.1	75.9 + 1.1	1.3 + 0.1
1250	14.9 + 1.5	5.1 + 0.7	0.5 + 0.1	78.2 + 1.2	1.3 + 0.1

b) In the Internal Surface of the External Cathodes

Surface finish aspects of the internal surface of the external cathodes processed in HCD are shown in Fig. 10. To emphasize the effects of the sputtering on the characteristics of the internal surface as a function of the processing temperatures, results are compared with the start surface condition (Fig. 10d), which was obtained by polishing. The results indicate the surface morphology is strongly modified. For low sintering temperature (1050 °C, Fig. 10a) a textured surface can be observed. The surface is characterized by the presence of very fine micrometer particles, which confirms the assumption of the obtainment of a sintered deposit layer with a typical morphology of powder particles, as previously indicated in the sintering time study, in accordance with the work of Romanowsky and Wronikowsky (1992).

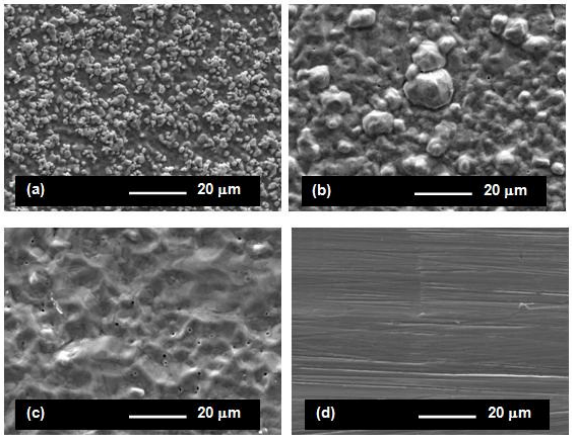

Figure 10. Surface finishing aspects of the internal surface of the external cathodes processed in HCD for sintering temperatures of: a) 1050 °C; b) 1150 °C; c) 1250 °C; and d) in the as non-processed condition.

Figure 11 shows a detailed view of the texture comprising very fine and homogeneous particles dispersion, obtained in the 1050 °C condition. The presence of irregular shape particles confirms the assumption that the round particles shape is actually related to the high processing temperature, as discussed. It is to be noted that the process of change from irregular to round particle shape at 1050 °C was only initiated, being observed some few very fine round particles on the surface. For sintering temperature of 1150 °C (Fig. 10b), the thermal activation was sufficiently high to provide not only the obtainment, but also the enlargement of the round particles. The increase of the sintering temperature resulted in particle growth and in a non-homogeneous particle dispersion (Fig. 10b), which could be associated to the particles coalescence phenomenon, as a consequence of an intense superficial diffusion activated by ion bombardment effect and the higher processing temperature, allied to the decrease of the surface free energy variation.

According to the chemical analysis of the internal surface of the external cathodes (Table 2), the increase in the Fe contents and consequent decrease in the amount of Cr, Ni, Si and Mn indicates that the Fe atoms sputtered from the pressed iron samples (see results discussed in Fig. 7) diffuse into the plasma and condense on the internal surface of the external cathode. It is to be noted the slight increment in the amount of iron atoms altering the chemical composition of the surrounding surface as the sintering temperature increases (1.8 at.% Fe and 2.3 at.% Fe, between 1050 and 1150 °C condition and between 1150 and 1250 °C condition, respectively).

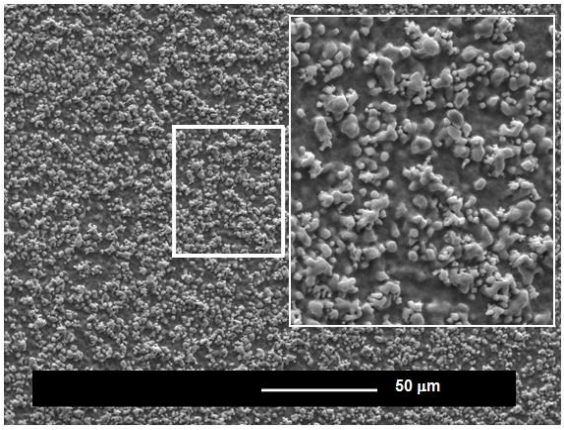

Figure 11. Detailed view of the texturing obtained in the internal surface of the external cathode processed in the 1050 °C condition.

So, it is necessary to explain the destination of the additional amounts of iron atoms sputtered from the sample surface, which comprise the exponential mass loss verified. Considering that the backscattered iron atoms which re-condense on the primitive surface do not take part in the mass loss characterization, the remainder necessarily have been lost along the discharge and condensed on the anode (thermal shield) surfaces. In such case, a considerably higher additional rate of iron atoms which condense on the internal surface of the external cathode could present re-sputtering phenomenon for the 1250 °C sintering temperature condition, as a consequence of its higher ton applied to the cathodes, which would explain the related fact.

Finally, the presence of argon in the composition of the processed surfaces is a strong indicative that the ions participate in the formation process of the condensed particles, in accordance with the proposed by Romanowsky and Wronikowsky (1992).

For the highest sintering temperature (1250 °C, Fig. 10c) new changes in the surface morphology can be observed. The particle texture observed for the smaller sintering temperature disappears.

Figure 12 shows Ra and Rz roughness measurements of the internal surfaces as a function of the sintering temperature, taken to evaluate the surface changes as a consequence of the sputtering effects on the external cathodes. The Ra and Rz values were 0.34, 0.62 and 0.44 μm, and 2.78, 4.96 and 3.64 μm for sintering temperatures of 1050, 1150 and 1250 °C, respectively. As expected, an increase in the sintering temperature from 1050 to 1150 °C (Fig. 10a, 10b) resulted in the increase for Ra and Rz values. The decrease of the Ra and Rz values for 0.44 and 3.64 μm, respectively, verified for surfaces processed with 1250 °C temperature (see Fig. 12) indicates the round-particle atoms tend to dissolve into surface.

Another event that occurs simultaneously is the re-sputtering of the particle atoms, since both the surfaces in the annular discharge is submitted to the ion bombardment effect. In accordance with the results verified for 1250 °C sintering temperature presented in Figs. 10(c) and 12, it is possible to assume the surface texturing process characterized by the occurrence of particle deposition could be assured for sintering temperatures up to 1150 °C.

Finally, for the highest sintering temperature (Fig. 10(c)), another characteristic tends to present at surface, since nanometric and micrometric porosity appears. This fact is probably related to the presence of argon atoms from the gaseous mixture dissolved into surface. In addition, the intense ion bombardment effect would tend to increase the point crystalline defects and an increment in the

vacancy density could be expected. The argon atom-vacancy pair diffusion could result in the coalescence of them at surface leading to the formation of new and small porous. This event would allow describing a new kind of surface texturing, which could be useful to store liquid lubricants and present beneficial effects of surface texturing, as that verified on mixed lubricated contacts, in accordance with Krupka et al. (2008) study.

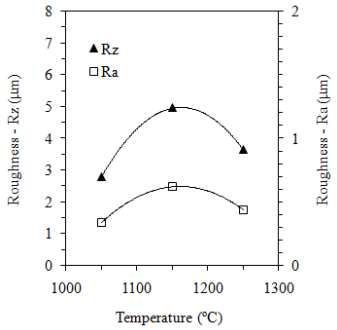

Figure 12. Ra and Rz roughness measurements of the internal surfaces of the external cathodes processed for different temperatures.

Conclusion

The results indicate that the sputtering mechanism in HCD sintering and texturing treatments can be adequately controlled as a function of the sintering time, comprising an important contribution to the development of green technologies for surface texturing, surface engineering, and part's sintering. The main conclusions can be listed as follows:

a) Strong modification of the surface finishing and morphology is evidenced in the samples as both the sintering time and temperature increase;

b) The sputtering effect tends to promote significant changes on the superficial pores' morphology, considering the start pores present at the pressed samples cylindrical surfaces, and the open pores tend to become closed as a consequence of the intense material transport mechanism verified for the metallic atoms, by interactions in plasma-surface system;

c) A tendency of surface modification in the pore size distribution could be expected increasing the sintering time, which would lead to a fine and disperse distribution of small open pores in the sintered samples. Otherwise, strong modification of the surface finishing and morphology is evidenced in the samples as the sintering temperature increases;

d) Despite the fact that obtainment of a fine and disperse distribution of small open pores in the sintered samples surface is dependent on the HCD ion bombardment effect (and so dependent on the electrical discharge parameters), it was evidenced that the success in closing open pores is strongly dependent on the start pore size and it is not only dependent on the sintering time and temperature;

e) Surface properties such as roughness and morphology can be altered as a function of sintering time and temperature in HCD, which make possible the obtainment of surface texturing as, simultaneously, the sintering process runs;

f) Surface finishing aspects and morphology of the internal surface of the external cathodes can be strongly modified. For short sintering times and low sintering temperatures, surface texturing characterized by the presence of dispersed and micrometer particles can be obtained. Otherwise, for long sintering times and high temperatures, the characteristic of the surface texturing process is changed, resulting in a roughened surface with the presence of nanometric and micrometric porosity;

g) Surface composition of the internal surface of the external cathodes can be successfully altered by deposition of metallic atoms sputtered from central cathode, and it is dependent on both the sintering time and temperature.

Acknowledgments

The author would like to thank the Brazilian Agency CNPq for financial support, and the M.Sc. V. Pimentel and M.Sc. J. W. Muller for the roughness profile measurements.

References

Basnyat, P., Luster, B., Muratore, C., Voevodin, A.A., Haasch, R., Zakeri, R., Kohli, P., Aouadi, S.M., 2008, "Surfacing texturing for adaptive solid lubrication". *Surface & Coatings Technology*, Vol. 203, pp. 73-79.

Benda M., Vlcek J., Cibulka V., Musil J., 1997, "Plasma Nitriding Combined With a Hollow Cathode Discharge Sputtering at High Pressures". *J. Vac. Sci. Technol. A*, Vol. 15, n. 5, pp. 2636-2643.

Brunatto, S.F., Khün, I., Muzart, J.L.R., 2005, "Surface Modification of Iron Sintered in Hollow Cathode Discharge Using an External Stainless Steel Cathode". *J. Phys. D: Appl. Phys.*, Vol. 38, pp. 2198-2203.

Brunatto S.F. and Muzart J.L.R., 2007, "Influence of the gas mixture flow on the processing parameters of hollow cathode discharge iron sintering". *J. Phys. D: Appl. Phys.*, Vol. 40, pp. 3937-3944.

Brunatto, S.F., Klein, A.N., Muzart, J.L.R., 2008, "Hollow Cathode Discharge: Application of a Deposition Treatment in the Iron Sintering", *J. of the Braz. Soc. of Mech. Sci. & Eng*. (ABCM), Vol. XXX, n. 2, pp. 145-151.

Gupta, P., Tenhundfeld, G., Daigle, E.O., Ryabkov, D., 2007, "Electrolytic plasma technology: Science and engineering – An overview". *Surface & Coatings Technology*, Vol. 201, pp. 8746-8760.

Koch, H. *et al.*, 1991, "Hollow Cathode Discharge Sputtering Device for Uniform Large Area Thin Film Deposition". *J. Vac. Sci. Technol. A*, Vol. 9, n. 4, pp. 2374-2377.

Kolobov, V.I., Tsendin, L.D., 1995, "Analytical Model of the Hollow Cathode Effect". *Plasma Sources Sci. Technol.*, Vol. 4, pp. 551-560.

Krupka, I., Vrbka, M., Hartl, M., 2008, "Effect of surface texturing on mixed lubricated non-conformal contacts". *Tribology International*, Vol. 41, pp. 1063-1073.

Muzart, J.L.R., Batista, V.J., Franco, C.V., Klein, A.N., 1997, "Plasma Sintering of AISI 316L Stainless Steel: The influence of the Processing Cycle on the Sample Density". Proceedings of Advances in Powder Metallurgy & Particulate Materials - MPIF, Part 3, pp. 77-84.

Romanowsky, Z., Wronikowski, M., 1992, "Specific Sintering by Temperature Impulses as a mechanism of Formation of a TiN Layer in the Reactive Pulse Plasma". *Journal of Materials Science*, Vol. 27, pp. 2619-2622.

Timanyuk V.A., Tkachenko V.M., 1989, "Study of a Glow Discharge in an Annular Cathode Cavity". *Sov. Phys. Tech. Phys.*, Vol. 34, n. 7, pp. 832-834.

V. Engel, A., 1994, "Ionized Gases". 2nd ed., American Institute of Physics, New York, USA, 325 p.